Nitrogen doped cuprous oxide as low cost hole-transporting material for perovskite solar cells

Han, Guifang; Du, Wen Han; An, Bao-Li; Bruno, Annalisa; Leow, Shin Woei; Soci, Cesare; Zhang, Sam; Mhaisalkar, Subodh Gautam; Mathews, Nripan

2018

Han, G., Du, W. H., An, B.-L., Bruno, A., Leow, S. W., Soci, C., . . . Mathews, N. (2018). Nitrogen doped cuprous oxide as low cost hole-transporting material for perovskite solar cells. Scripta Materialia, 153, 104-108. doi:10.1016/j.scriptamat.2018.04.049

https://hdl.handle.net/10356/141529

https://doi.org/10.1016/j.scriptamat.2018.04.049

Nitrogen doped cuprous oxide as low cost hole-transporting material for perovskite solar cells

Guifang Han [a,1], Wen Han Du [b,c,1], Bao-Li An [d], Annalisa Bruno [a], Shin Woei Leow [c], Cesare Soci [e], Sam Zhang [f], Subodh G. Mhaisalkar [a,c], Nripan Mathews [a,c]*

[a] Energy Research Institute @NTU (ERI@N), Nanyang Technological University, Research Techno Plaza, X-Frontier Block, Level 5, 50 Nanyang Drive, 637553, Singapore

[b] Changzhou Institute of Technology, Changzhou, Jiangsu 213002, P.R. China

[c] School of Materials Science and Engineering, Nanyang Technological University, Nanyang Avenue, 639798, Singapore

[d] Department of Chemistry, College of Science, Shanghai University, Shanghai, 200444, P.R. China

[e] Division of Physics and Applied Physics, School of Physical and Mathematical Sciences, Nanyang Technological University, 21 Nanyang Link, 637371, Singapore

[f] Faculty of Materials and Energy, Southwest University, Chongqing 400715, China

[1] These authors contribute equally to this work

[*] Corresponding author (N.M.). E-mail address: Nripan@ntu.edu.sg

KEYWORDS: Perovskite, solar cell, hole-transporting material, amorphous, nitrogen doped cuprous oxide

ABSTRACT:

Substituting expensive traditional hole transporting material (HTM) with cheaper inorganics is a key factor for perovskite photovoltaics commercialization. Cu_2O is a promising *p*-type semiconductor exhibiting good band-alignment with perovskite. However, due to solvent and temperature incompatibility, Cu_2O is typically employed in inverted configuration, where an even more expensive, unstable Phenyl-C61-butyric acid methyl ester is necessary as an electron-transporting layer. Therefore, we explored the use of sputtered nitrogen-doped Cu_2O directly on halide-perovskite as a HTM. With a thin interfacial layer, efficiency of 15.73% was achieved. This work indicates the possibility of low cost sputtered inorganics as HTM for efficient perovskite photovoltaics.

Organic-inorganic halide perovskite solar cell has opened a new era for high efficiency solution processed thin film photovoltaics [1-5]. Efforts in composition design [6, 7], process modification [8], investigation of dominant recombination mechanism [9, 10] and therefore strategies to improve the performance of perovskite solar cells [11], have led to a record power conversion efficiency more than 22 %. A typical perovskite solar cell architecture consists of electron transporting layer, perovskite absorber and hole transporting material layered either in a conventional or an inverted configuration [1, 12]. The perovskite absorber layer as well as the hole-transporting layer, (typically Spiro-MeOTAD), can be solution processed by simple spin coating. However, the high cost of Spiro-MeOTAD poses a major obstacle in the path of large-scale commercialization of perovskite solar cells [13]. Inorganic *p*-type semiconductors, especially Cu-

based materials such as copper iodide (CuI), copper thiocyanate (CuSCN), and cuprous oxide (Cu_2O) [14-16], has recently attracted significant attention as hole-transporting materials (HTM) owing to their high mobility and low fabrication cost. CuI is the first reported inorganic Cu-based HTM for perovskite solar cell but achieved a low efficiency of ~6%. CuSCN has been reported recently as HTM to obtain a power conversion efficiency of more than 20% with a better stability [15]. However, not many solvents are available that could readily dissolve CuSCN. Diethyl sulfide which is presently utilized, is not environmentally benign and also has an affinity to dissolve perovskite requiring careful processing. Cu_2O has been investigated for many years due to its unique *p*-type semiconducting properties. Appropriate energy band alignment along with its low cost and environmental friendliness makes Cu_2O an excellent candidate as HTM for perovskite solar cells. Cu_2O has been reported successfully as an HTM for perovskite in inverted structure with Phenyl-C61-butyric acid methyl ester (PCBM) as electron transporting layer on top [17-20]. The Cu_2O is firstly deposited on Indium tin oxide substrate using solution process such as successive ionic layer absorption and reaction, or spin coating using $Cu(acac)_2$ as the precursor [17, 18]. Subsequently, the perovskite is spun coated on the Cu_2O layer, followed by a PCBM electron transport layer. This inverted (*p-i-n*) configuration is utilized due to the tendency of the Cu_2O deposition processes to degrade the perovskite layer below it due to the solvents or the temperatures applied. PCBM, in addition to being less cost-effective than Spiro-MeOTAD, is also not stable at ambient atmosphere. Another limitation is the optical absorption that could happen in the Cu_2O when applied in the inverted configuration. Cu_2O with a bandgap of around 2.21 eV [20], will absorb light with wavelength less than 560nm, which will decrease the light absorption in perovskite. All these factors dramatically weaken the advantage of using Cu_2O as HTM for perovskite solar cells in an inverted configuration. Therefore, the best way to use Cu_2O is to

directly or partially substitute the Spiro-MeOTAD layer in a conventional perovskite solar cell configuration. Magnetron sputtering is a promising technique to fabricate uniform, dense and pin-hole free film without considering the issues of solvent compatibility [21]. However the heat generated and the kinetic energy of the atoms in the sputtering may affect the perovskite layer and hence the performance of devices. Ahmadi et al. carefully adjusted the tilting angle of substrate against the sputtering target and obtained a uniform and compact Cu_2O film on top of perovskite layer with a device efficiency of 8.93% [22]. Since most commonly used HTMs, including inorganics and organics, have relatively poor conductivity, doping has been proved to be an effective approach to improve their carrier densities. Y. Zhou et al. [23] has thoroughly reviewed how doping and alloying improves the electronic properties of electron and hole transporting materials and further the perovskite solar cell performance. Nitrogen (N) has been reported as an effective *p*-type dopant for Cu_2O. It is generally believed that N substitutes the oxygen sites (N_O). Recently theoretical calculations have proposed that N_O is a deep acceptor and is unlikely to be the cause of observed increasing of hole concentration [24, 25]. Careful defect physics calculation suggested that N_2 molecule on Cu's site $(N_2)_{Cu}$ is a shallow acceptor with a low formation energy, which might give hole carriers [24]. This is further confirmed experimentally by electron energy loss spectroscopy revealing that nitrogen is in molecular N_2 form in Cu_2O [26]. In this work, we have lowered the sputtering power to avoid damage of perovskite layer and introduced nitrogen doping to further explore Cu_2O as HTM for enhanced solar cell performance resulting in an efficiency of 15.73%.

To avoid strong damage of perovskite films during the sputtering, a low sputtering power of 15W (the lowest power attainable in the deposition system) is used for the deposition of all CuO_xN_y films. Performance of devices fabricated with low power sputtered CuO_xN_y (~180 nm) on the

halide perovskite layer is presented in **Fig. S1**. The open-circuit voltage (V_{oc}) is around 0.8V; short-circuit current (J_{sc}) is less than 5 mA/cm^2 and power conversion efficiency (PCE) is lower than 2%. The current-voltage (*I-V*) curve of best cell is given in **Fig. S1(b)** with a PCE of 1.54%. Although low power is applied during sputtering, it is still not able to form a good interface between perovskite and CuO_xN_y. There is no noticeable physical damage observable in the cross section microstructure, as can be seen from **Fig. S2**, indicating that the defects are electronic in nature. To manage the interface, a thin layer of Spiro-MeOTAD is introduced between perovskite and CuO_xN_y as a buffer layer. The device performance shown in **Fig. S3** shows a dramatic improvement. The influence of gas composition on the properties of the solar cell was then studied. We fixed the flow rate of oxygen (O_2) and varied the flow rate of nitrogen (N_2). With increasing N_2 flow rate, there is a reduction in the V_{oc} , J_{sc} and fill factor (*FF*). The highest efficiency of 13.42% is achieved with an O_2:N_2 flow rate of 2:2, the lowest N_2 flow rate. Then the N_2 flow rate was set at 2 sccm and the O_2 flow rate varied between 0.5, 1 to 2 sccm. Further decrease of the O_2 flow rate resulted in the appearance of zero valence copper. When decreasing the flow rate of O_2, increase in V_{oc} and *FF* is observed with a slight decrement of J_{sc}. The highest overall efficiency (15.73%) is achieved with a lower O_2 flow rate of 0.5 sccm, as shown in **Fig. 1**. The higher V_{oc} obtained with less O_2, might be due to a more favorable band alignment with the small change in stoichiometry of CuO_xN_y films. When comparing the effect of N-doping at same O_2 flow of 0.5 sccm, although the *FF* didn't change so much, the overall efficiency is reduced by more than 1% against N-doped cuprous oxide as the HTM primarily due to lower J_{sc} and V_{oc}.

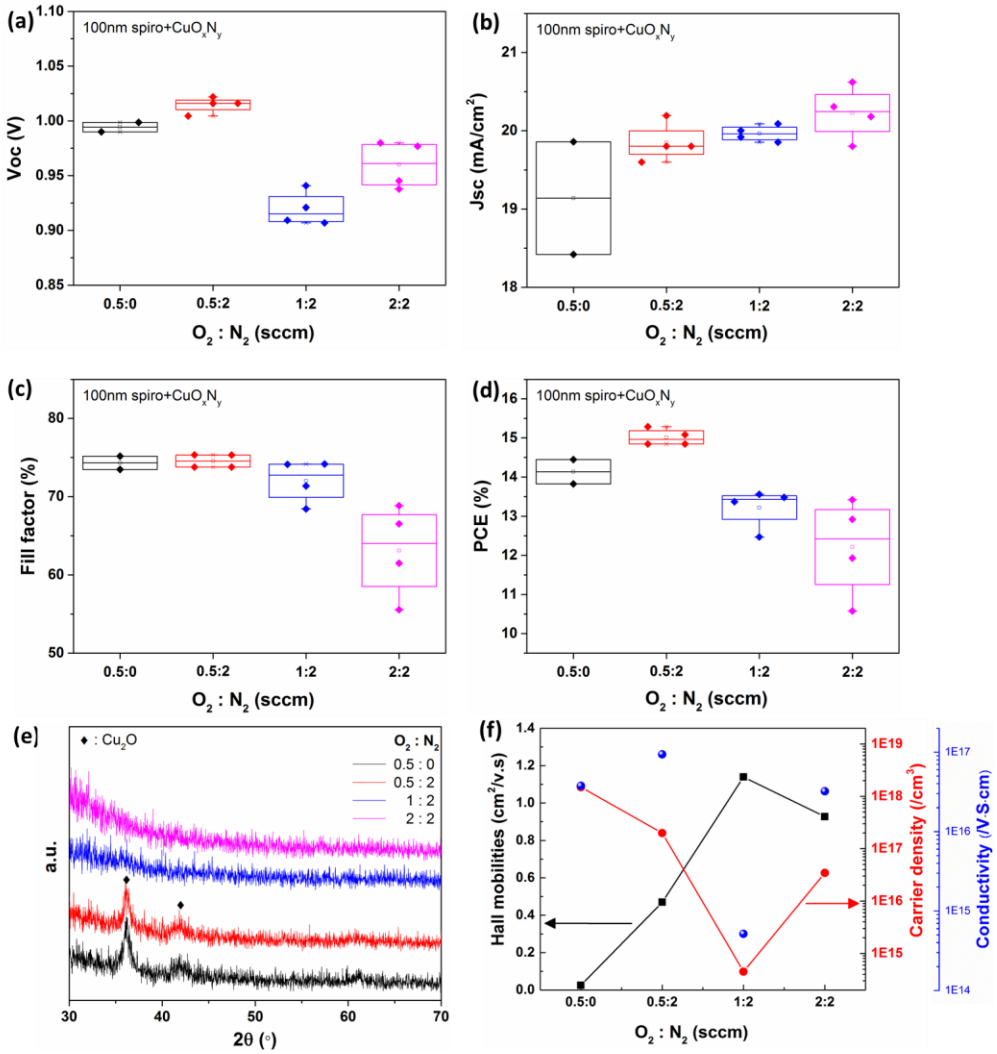

Fig. 1 Device performance distribution of characteristic photovoltaic parameters obtained from perovskite based solar cell with CuO_xN_y as hole transporting materials deposited at different O_2:N_2 ratio: (a) open-circuit voltage (V_{oc}), (b) short-circuit current density (J_{sc}), (c) fill factor (*FF*) and (d) power conversion efficiency (PCE) at similar device fabrication conditions. 100nm-thick Spiro-MeOTAD was used as interfacial and protection layer during CuO_xN_y sputtering. (e) XRD spectrums and (f) Hall mobility, carrier density and conductivity of sputtered CuO_xN_y films with different O_2:N_2 flow ratio.

The X-ray diffraction patterns of CuO_xN_y sputtered with different O_2:N_2 ratio are illustrated in Fig. 1(e). It clearly indicates that with low O_2 flow rate of 0.5sccm, Cu_2O phase is formed. However, with further increase in the O_2 flow rate, the CuO_xN_y films becomes amorphous. Interestingly, better device performance is obtained with low O_2 flow rate. This might due to the

better crystallinity of the CuO_xN_y films. To further understand the correlation of device performance with the properties of CuO_xN_y films, mobility and carrier density were investigated from Hall measurement are shown in **Fig. 1(f)**. The Hall mobility (black line) increased with the addition of nitrogen reaching a maximum at O_2:N_2 ratio of 1:2. However, the carrier density (red line) exhibits the opposite trend. Based on these factors, the film conductivity was calculated and plotted in blue (**Fig. 1(f)**). The highest conductivity is obtained with an O_2:N_2 ratio of 0.5:2, which is consistent with higher crystallinity of CuO_xN_y films and the corresponding devices performance. The microstructure of sputtered CuO_xN_y films (Fig. S4) show no significant difference for different O_2:N_2 ratios. Therefore, the crystallinity and electronic properties of CuO_xN_y films are more critical for device performance.

With the O_2:N_2 ratio fixed at 0.5:2, we examine the effect of CuO_xN_y thickness on the performance of the perovskite solar cell. From **Fig. 2(a)**, the PCE of the perovskite cells peaks at 80nm CuO_xN_y thickness and decreases subsequently. Based on this optimized condition, 20 devices were fabricated to verify the reproducibility of this process as shown in **Fig. 2(b)**. The efficiency of all devices exhibits a narrow distribution within the range of 14% to 15%, with an average value of 14.70%. The current-voltage (*I-V*) curve of the champion cell is given in **Fig. 2(c)**, demonstrated a V_{oc} of 1.04V, J_{sc} of 19.84 mA/cm^2, *FF* of 75.87% and efficiency of 15.73%, significantly higher than the reported value of 8.93% [22] with sputtered cuprous oxide. The incident photon-to-current efficiency (IPCE) measurement indicates around 80% quantum efficiency with an integrated current density of 19.45 mA/cm^2, which matches well with the *I-V* measurement (**Fig. 2(d)**).

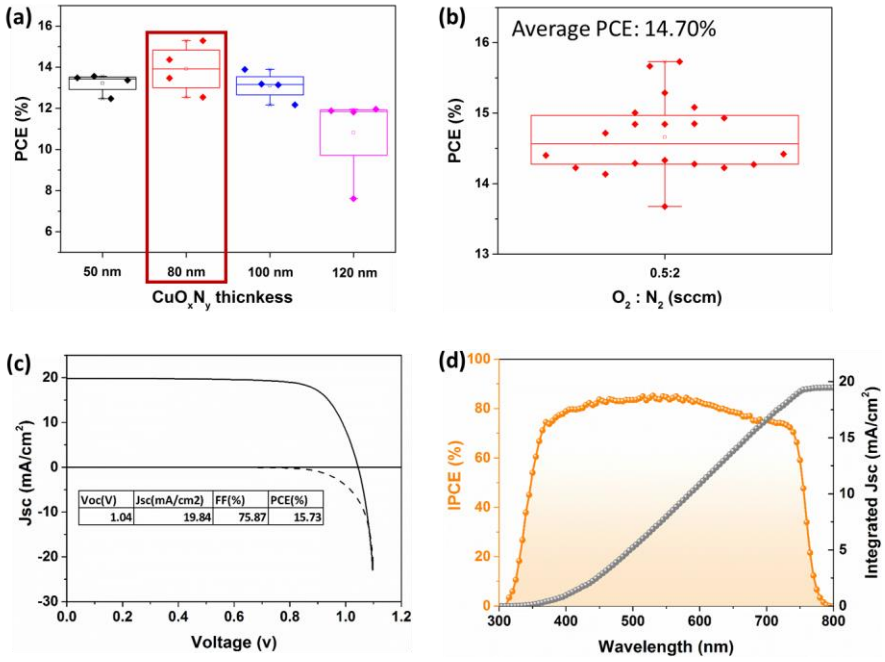

Fig. 2 (a) Power conversion efficiency (PCE) of devices with different thickness of CuO_xN_y, in which the 80nm devices give the highest PCE; (b) PCE distribution of perovskite solar cells with Spiro-MeOTAD /CuO_xN_y as hole transporting materials fabricated at optimal condition; (c) Characteristic current density (J_{sc}) vs voltage (V) curves of the champion cell fabricated using Spiro-MeOTAD/CuO_xN_y as hole transporting materials; (d) Incident photon-to-current efficiency (IPCE) of best performing device with integrated current density of 19.45 mA/cm^2

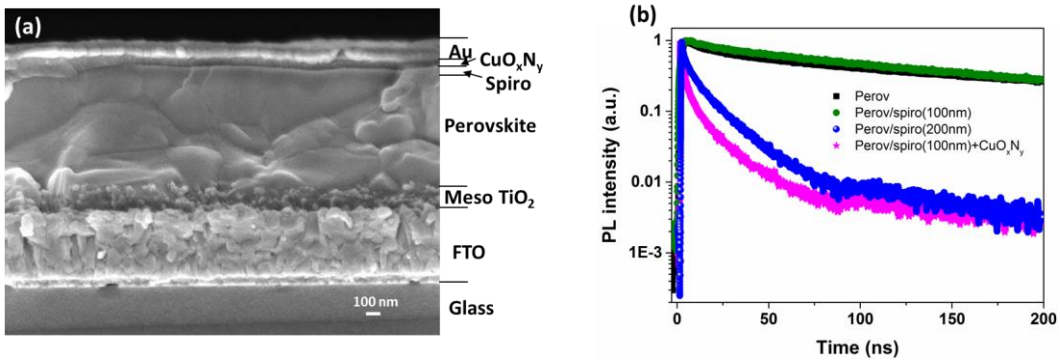

Fig. 3 (a) Field emission scanning electron microscopy (FESEM) images of the cross-section of typical perovskite solar cell; (b) Time resolution photoluminescence (TRPL) analysis of perovskite films with different hole transporting layers, lifetime is calculated by fitting the data with bi-exponential equation of $y = y_0 + A_1 e^{-(x-x_0)/t1} + A_2 e^{-(x-x_0)/t2}$

From a cross section of the microstructure (**Fig. 3(a)**), the capping layer of perovskite on top of mesoporous TiO_2 is around 500nm. This is followed by a thin ~100nm layer of Spiro-MeOTAD with no clear interface to the perovskite layer below. The CuO_xN_y layer grows in a columnar microstructure (seen more clearly at increased thickness, as in **Fig. S5**) with good adhesion to the Spiro-MeOTAD layer, likely facilitating charge transport.

To further investigate the working mechanism, time resolved photoluminescence (TRPL) was performed on perovskite films with and without different HTM layers. A bi-exponential decay equation of $y = y_0 + A_1 e^{-(x-x_0)/t1} + A_2 e^{-(x-x_0)/t2}$ is employed to fit the measured data (**Fig. 3(b)**) and the extracted exciton lifetimes are listed in **Table S1**. Bare perovskite film on glass gives a fluorescence lifetime of 484ns, which signifies good quality film. When a layer of 100nm-thick Spiro-MeOTAD is added on top, the fluorescence lifetime decreases to 262ns, suggesting charge separation at the interface is taking place. Possibly due to the thin Spiro-MeOTAD layer, hole transport is not very efficient. When the Spiro-MeOTAD layer thickness is increased to 200nm (which is the thickness for normal devices), the lifetime dramatically decreases to 15ns, indicating efficient quenching due to better charge extraction by this thicker Spiro-MeOTAD layer. Interestingly, when 100nm-thick Spiro-MeOTAD and sputtered CuO_xN_y are used as the HTM, the fluorescence lifetime is just 11ns, even lower than that with 200nm Spiro-MeOTAD. This result provides strong support that CuO_xN_y combined with a thin layer of Spiro-MeOTAD is an efficient hole acceptor for perovskites.

In summary, we have investigated the usage of nitrogen doped amorphous cuprous oxide as a hole transporting material for perovskite solar cells. The highest efficiency of 15.73% is achieved with nitrogen doped low power sputtered CuO_xN_y and a thin Spiro-MeOTAD interfacial layer, which is much higher than the reported value of 8.93% with similar process. Time resolved

photoluminescence and Hall measurements confirmed the efficient charge transfer between perovskite and CuO_xN_y-based HTL, and high conductivity of nitrogen doped cuprous oxide. This work demonstrates the first successful case of using sputtered cuprous oxide as a cheaper and efficient hole transporting material for perovskite solar cell. However, further work on the interface should be performed to eventually eliminate the usage of the interfacial modifier.

Acknowledgements

The authors acknowledge funding from the National Research Foundation, Prime Minister's Office, Singapore under its Competitive Research Program (CRP Award No. NRF-CRP14-2014-03) and through the Singapore-Berkeley Research Initiative for Sustainable Energy (SinBeRISE) CREATE Program; Nanyang Technological University start-up grants (M4080514 and M4081293); the Ministry of Education Academic Research Fund Tier 1 grants (RG184/14, RG166/16 and RG101/15), and Tier 2 grants (MOE2016-T2-1-100, MOE2014-T2-1-044, MOE2015-T2-2-015 and MOE2016-T2-2-012).

References

[1] G. Han, S. Zhang, P.P. Boix, L.H. Wong, L. Sun, S.-Y. Lien, Prog. Mater Sci. 87 (2017) 246-291.
[2] T.C. Sum, N. Mathews, Energy Environ. Sci. 7(8) (2014) 2518-2534.
[3] H.J. Snaith, J. Phys. Chem. Lett. 4(21) (2013) 3623-3630.
[4] H.S. Jung, N.G. Park, Small 11(1) (2015) 10-25.
[5] T.M. Brenner, D.A. Egger, L. Kronik, G. Hodes, D. Cahen, Nature Rev. Mater. 1 (2016) 15007.
[6] N.J. Jeon, J.H. Noh, W.S. Yang, Y.C. Kim, S. Ryu, J. Seo, S.I. Seok, Nature 517(7535) (2015) 476-480.
[7] M. Saliba, T. Matsui, J.-Y. Seo, K. Domanski, J.-P. Correa-Baena, N. Mohammad K, S.M. Zakeeruddin, W. Tress, A. Abate, A. Hagfeldt, M. Gratzel, Energy Environ. Sci. 9(6) (2016).
[8] N. Ahn, D.-Y. Son, I.-H. Jang, S.M. Kang, M. Choi, N.-G. Park, J. Am. Chem. Soc. 137(27) (2015) 8696-8699.

[9] B. Wu, H.T. Nguyen, Z. Ku, G. Han, D. Giovanni, N. Mathews, H.J. Fan, T.C. Sum, Adv. Energy Mater. 6 (2016) 1600551.
[10] I. Zarazua, G. Han, P.P. Boix, S. Mhaisalkar, F. Fabregat-Santiago, I. Mora-Seró, J. Bisquert, G. Garcia-Belmonte, J. Phys. Chem. Lett. 7 (2016) 5105-5113.
[11] G. Han, T.M. Koh, S.S. Lim, T.W. Goh, X. Guo, S.W. Leow, R. Begum, T.C. Sum, N. Mathews, S. Mhaisalkar, ACS Appl. Mater. Interfaces 9(25) (2017) 21292-21297.
[12] Released by National Renewable Energy Laboratory (2018).
[13] Y. Rong, L. Liu, A. Mei, X. Li, H. Han, Adv. Energy Mater. 5 (2015) 1501066.
[14] A.S. Subbiah, A. Halder, S. Ghosh, N. Mahuli, G. Hodes, S.K. Sarkar, J. Phys. Chem. Lett. 5(10) (2014) 1748-53.
[15] P. Qin, S. Tanaka, S. Ito, N. Tetreault, K. Manabe, H. Nishino, M.K. Nazeeruddin, M. Gratzel, Nat. Commun. 5 (2014) 3834.
[16] N. Arora, M.I. Dar, A. Hinderhofer, N. Pellet, F. Schreiber, S.M. Zakeeruddin, M. Grätzel, Science (2017).
[17] J.A. Christians, R.C. Fung, P.V. Kamat, J. Am. Chem. Soc. 136(2) (2014) 758-64.
[18] S. Chatterjee, A.J. Pal, J. Phys. Chem. C 120(3) (2016) 1428-1437.
[19] H. Rao, S. Ye, W. Sun, W. Yan, Y. Li, H. Peng, Z. Liu, Z. Bian, Y. Li, C. Huang, Nano Energy 27 (2016) 51-57.
[20] W. Sun, Y. Li, S. Ye, H. Rao, W. Yan, H. Peng, Y. Li, Z. Liu, S. Wang, Z. Chen, L. Xiao, Z. Bian, C. Huang, Nanoscale 8(20) (2016) 10806-10813.
[21] W. Yu, F. Li, H. Wang, E. Alarousu, Y. Chen, B. Lin, L. Wang, M.N. Hedhili, Y. Li, K. Wu, X. Wang, O.F. Mohammed, T. Wu, Nanoscale 8(11) (2016) 6173-6179.
[22] W. Du, J. Yang, C. Xiong, Y. Zhao, X. Zhu, Int. J. Mod Phys B 31(16-19) (2017) 1744065.
[23] Y. Zhou, Z. Zhou, M. Chen, Y. Zong, J. Huang, S. Pang, N.P. Padture, J. Mater. Chem. A 4(45) (2016) 17623-17635.
[24] J. T-Thienprasert, S. Limpijumnong, Appl. Phys. Lett. 107(22) (2015) 221905.
[25] Z. Zhao, X. He, J. Yi, C. Ma, Y. Cao, J. Qiu, RSC Advances 3(1) (2013) 84-90.
[26] Y. Wang, J. Ghanbaja, D. Horwat, L. Yu, J.F. Pierson, Appl. Phys. Lett. 110(13) (2017) 131902.

Supporting Information

Nitrogen doped amorphous cuprous oxide as low cost hole-transporting material for perovskite solar cells

*Guifang Han [a,1], Wen Han Du [b,c,1], Bao-Li An [d], Annalisa Bruno [a], Shin Woei Leow [c], Cesare Soci [e], Sam Zhang [f], Subodh G. Mhaisalkar [a,c], Nripan Mathews [a,c]**

- **Materials and methods**

Film and device fabrication

Fluorine doped tin oxide (FTO) substrates were etched using Zn powder and 2M hydrochloric acid (HCl). The etched FTO substrates and glass slides were subsequently cleaned with Decon soap solution, deionized water and finally with ethanol. A thin compact layer of TiO_2 was deposited using a solution of titanium diisopropoxide bis(acetylacetonate) (75 wt% in isopropanol) and absolute ethanol (ratio 1:9 by volume) by spray-pyrolysis at 450°C on FTO substrates. A mesoporous TiO_2 film was deposited by spin-coating TiO_2 paste (30 NR-D, Dyesol) diluted with ethanol (1:5.5 w/w) on the substrate and calcined at 500°C for 30 min. Then 0.1M bis(trifluoro-methane)sulfonimide lithium salt (Li-TFSI) in acetonitrile was spin coated to dope mesoporous TiO_2 according to the report by F. Giordano et al [1]. The doped substrates were

annealed at 450°C for 30 min and then transferred into N_2 filled glove box immediately after cooling to 150°C.

FAI and MABr were purchased from GreatCell Solar, Australia. PbI_2 and $PbBr_2$ are from Tee Hai Chem Pte Ltd, Japan, and all the other chemicals are from Sigma Aldrich. A mixed solution of FAI (1M), PbI_2 (1.1M), MABr (0.2M) and $PbBr_2$ (0.2M) were dissolved in dimethylformamide: dimethyl sulfoxide 4:1(v:v) with excess PbI_2. 1.5 M CsI stored solution were added into the mixed solution forming the composition of $(FA_{0.83}MA_{0.17})_{0.95}Cs_{0.05}Pb(I_{0.83}Br_{0.17})_3$. The perovskite layer was deposited by single step method as reported in literature [2]. In brief, the triple cation solution was spin-coated on the substrate with a two steps deposition method i.e. at 1000 rpm for 10 s and 6000 rpm for 30 s respectively. During the second step, 100 µL chlorobenzene was dropped on the spinning substrate after 15 s. The substrates were subsequently annealed at 100 °C for 60 min. For film characterization, perovskites films were prepared on the glass substrate.

Spiro-OMeTAD solution (35 mg/mL in chlorobenzene) prepared using Lithium bis(trifluoromethylsulfonyl) imide, tert-butylpyridine and cobalt dopant, and was spin coated on the top of the perovskite films at 4000 rpm for 30s.

CuO_x thin films with different thickness were prepared by radio frequency sputtering technique. 2 inch high purity (99.999%) Cu plate was used as the sputter target. The target to substrate distance was kept at 13cm, and the substrate temperature was kept at room temperature, the process pressure was fixed at 3mTorr with different gas ratios between Ar and O_2/N_2. The sputter power was fixed at 15W for solar cell application, and changed to 50W to test the crystalline structure changes.

Gold counter electrode was deposited using thermal evaporation method.

Characterization

The crystallographic information of the perovskite films were analyzed by Panalytical XPert Pro X-Ray diffractometer with Cu Kα radiation and a step of 0.02°. Thickness of the CuO_x was measured by step profiler and calibrated by cross-section SEM image. The cross sectional image of device and films were recorded by using Field Emission Scanning Electron Microscopy (FESEM, JEOL, JSM 7600F).

For the photovoltaic measurements, all devices (0.25 cm^2 active area) were measured by using solar simulator (San-EI Electric, XEC-301S) under AM 1.5G standard with a 0.09 cm^2 metal mask. Current-voltage (*J*-*V*) characteristics were recorded with a Keithley (model 2612A) digital source meter.

Carrier lifetime of perovskite films with different additives on glass substrates were measured using time resolved photoluminescence (TRPL) analysis. The system consists of a microscope based PL setup with an excitation and emission collection path from the same side. The measurements were realized using a VIS-NIR microscope objective (10x, NA=0.65). Light excitation was provided by laser diodes at 405 nm (Pico Quant LDH Series P-C-405B) with 60 picosecond pulse duration and 40 MHz repetition rate. The beam spot size was about 2 μm. The signal from the Single Photon Avalanche Diode (Laser 2000, Model $PD-50-CTE) detector was acquired by a time-correlated single photon counting card.

Alternating current Hall measurement is conducted to verify the mobility and carrier density.

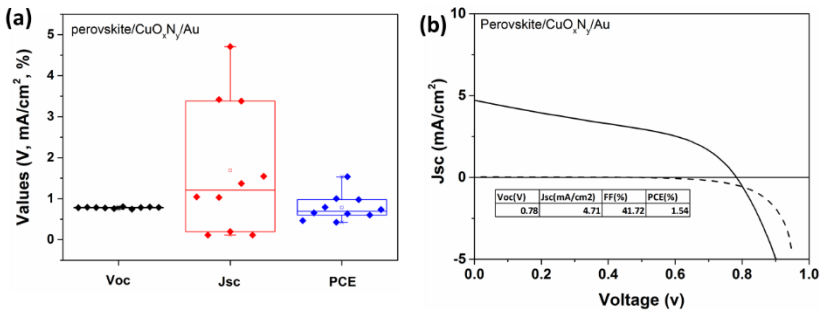

Figure S1 (a) Devices performance distribution of perovskite solar cells with a configuration of FTO/TiO_2(blocking layer)/meso TiO_2/perovskite/CuO_xN_y/Au, where CuO_xN_y is directly sputtered on top of perovskite; (b) Typical current density-voltage (I-V) curve of this device.

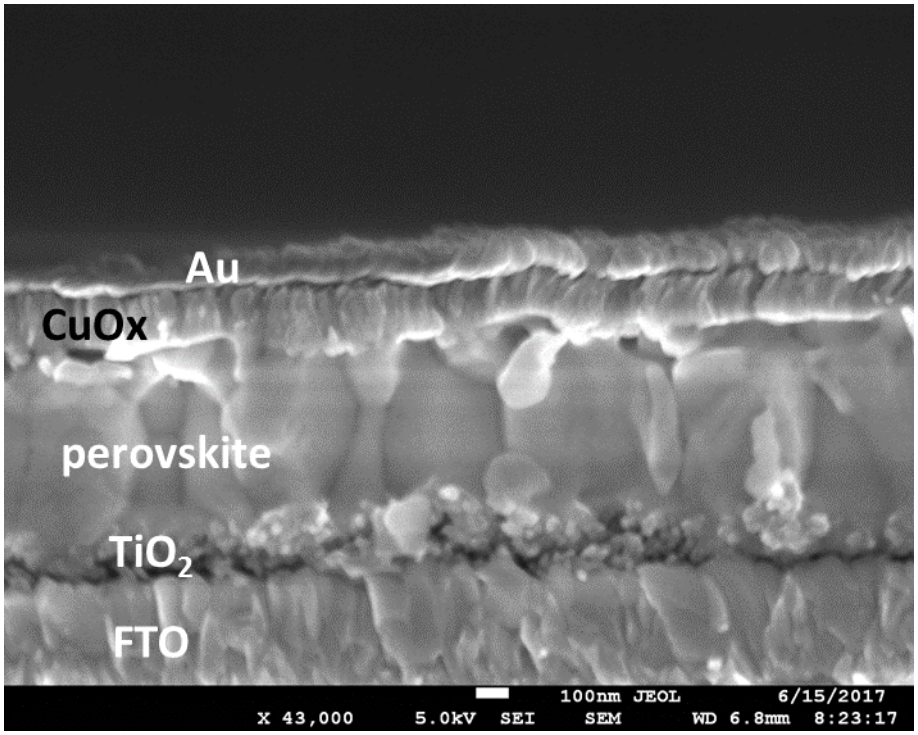

Figure S2 Cross-section SEM image of perovskite device with sputtered CuO_x as hole transporting material

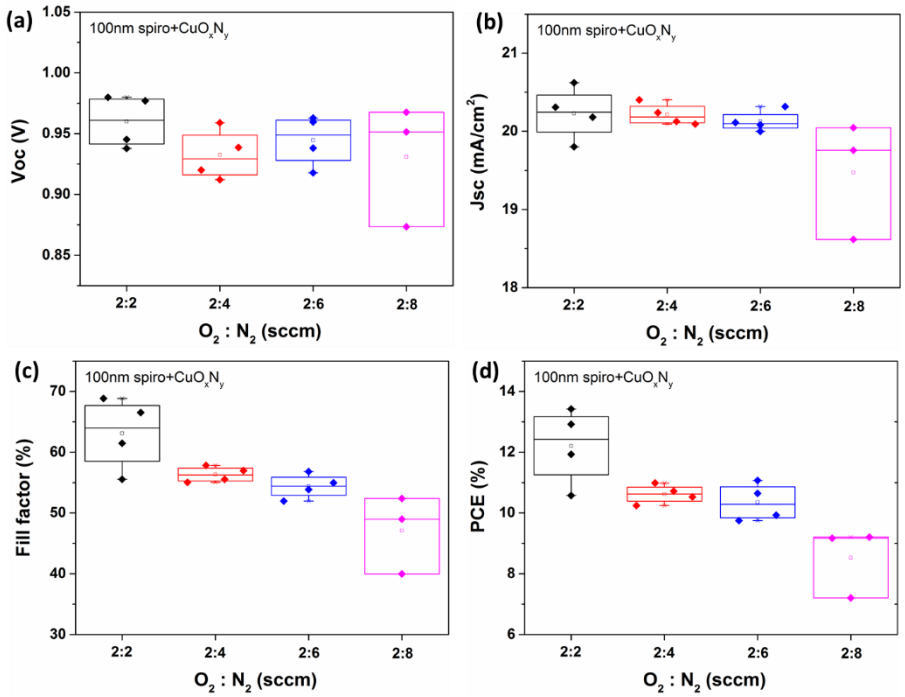

Figure S3 Device performance distribution of characteristic photovoltaic parameters obtained from perovskite based solar cell with CuOxNy as hole transporting materials deposited at fixed O_2 flow and different N_2 flow rate: (a) open-circuit voltage (Voc), (b) short-circuit current density (Jsc), (c) fill factor (FF) and (d) power conversion efficiency (PCE) at similar device fabrication conditions. 100nm-thick spiro was used as interfacial and protection layer during CuO_xN_y sputtering.

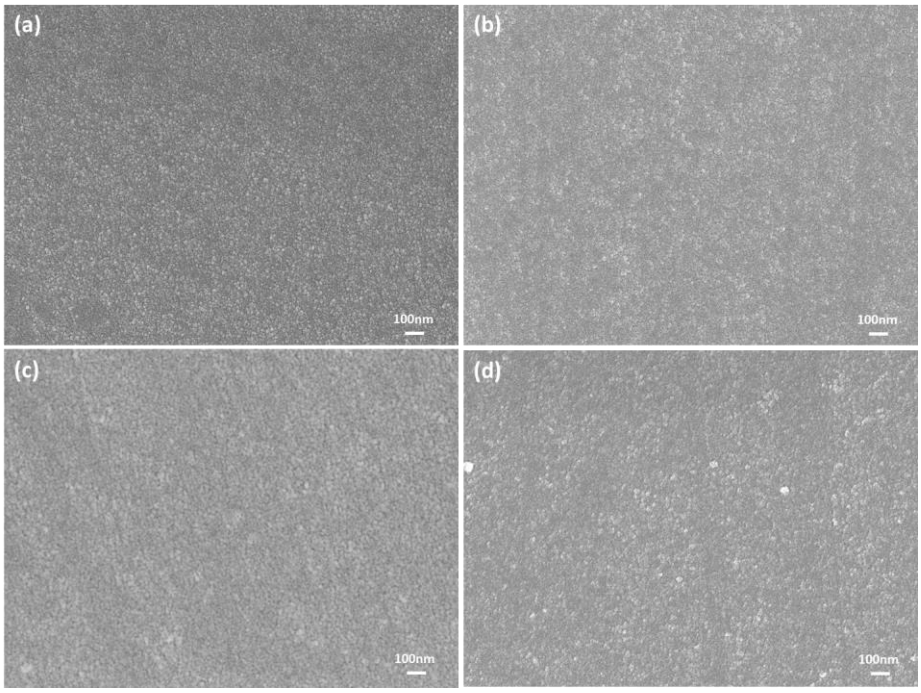

Figure S4 SEM microstructure of CuO_xN_y sputtered at O_2:N_2 ratio of (a) 0.5:0, (b) 0.5:2, (c) 1:2 and (d) 2:2.

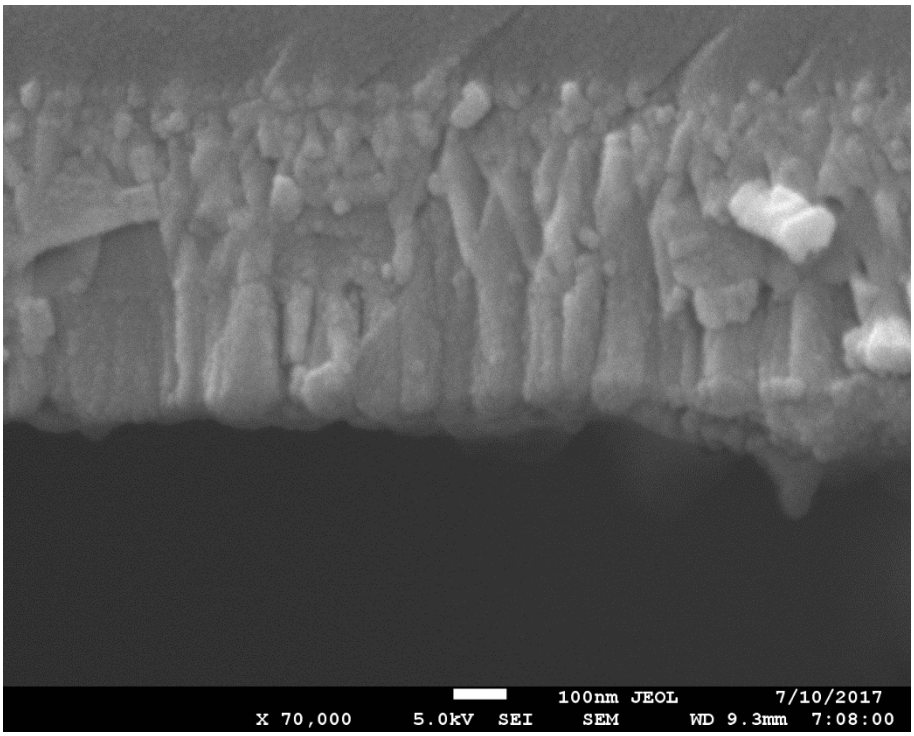

Figure S5 Cross-section microstructure of sputtered thicker Cu_2O film with column-like structure

Table S1 Calculated charge carrier lifetime of perovskite film with/without different hole transporting layers

Materials	Perovskite	Perovskite/spiro (100nm)	Perovskite/spiro (200nm)	Perovskite/spiro (100nm)+CuO_xN_y
A_1	0.47	0.40	0.51	0.74
t_1 (ns)	51	55	2	1
A_2	0.53	0.60	0.49	0.26
t_2 (ns)	484	262	15	11

References

[1] F. Giordano, A. Abate, J.P. Correa Baena, M. Saliba, T. Matsui, S.H. Im, S.M. Zakeeruddin, M.K. Nazeeruddin, A. Hagfeldt, M. Graetzel, Nat Commun 7 (2016) 10379.
[2] M. Saliba, T. Matsui, J.-Y. Seo, K. Domanski, J.-P. Correa-Baena, N. Mohammad K, S.M. Zakeeruddin, W. Tress, A. Abate, A. Hagfeldt, M. Gratzel, Energy Environ. Sci. 9(6) (2016).